2021 43rd Annual International Conference of the
IEEE Engineering in Medicine & Biology Society (EMBC)
Oct 31 - Nov 4, 2021. Virtual Conference

Multi-contrast multi-shot EPI for accelerated diffusion MRI

Banafshe Shafieizargar[1], Ben Jeurissen[1], Dirk H.J. Poot[2], Arnold J. den Dekker[1] and Jan Sijbers[1,3]

Abstract— **The clinical application of diffusion MRI is practically hindered by its long scan time. In this work, we introduce a novel imaging and parameter estimation framework for time-efficient diffusion MRI. To improve the scan efficiency, we propose ADEPT (Accelerated Diffusion EPI with multi-contrast shoTs), in which diffusion contrast settings are allowed to change between shots in a multi-shot EPI acquisition (i.e. intra-scan modulation). The framework simultaneously corrects for artifacts related to shot-to-shot phase inconsistencies in multi-shot imaging by iteratively estimating the phase map parameters along with the diffusion model parameters directly from the acquired intra-scan modulated k-space data. Monte Carlo simulation experiments show the effective estimation of diffusion tensor parameters in multi-shot EPI diffusion imaging.**

I. INTRODUCTION

Diffusion Magnetic Resonance Imaging (dMRI) is a powerful, non-invasive technique that is able to infer tissue microstructure at the cellular level by probing the random microscopic motion (i.e., diffusion) of water molecules. In conventional quantitative dMRI, spatial maps of diffusion parameters are estimated from multiple diffusion-weighted (DW) images with different diffusion sensitizing gradient strengths and directions. It relies on a two-step procedure. First, a set of differently diffusion weighted images are reconstructed individually. Secondly, a diffusion model is fitted voxel-wise to the resulting set of DW images. Since many DW images are currently required for accurate and precise diffusion parameter estimation, dMRI suffers from a long scan time thereby limiting patient throughput and comfort. Hence, there is a strong need for scan time reduction.

In recent years, advanced reconstruction methods have been developed for dMRI that allow scan time reduction by intermixing spatial frequency encoding with diffusion weighting (i.e. by sampling the k-q space). In these approaches, the intermediate step of the image reconstruction is avoided by combining the image reconstruction and parameter estimation steps in an integrated single-step parameter estimation framework that allows to estimate the diffusion parameter maps directly from the k-q-space data [1], [2]. Such joint reconstruction and estimation framework can be used in combination with fast acquisition schemes such as multi-shot echo-planar imaging (EPI) to reduce the acquisition time of dMRI [3]. Multi-shot diffusion weighted imaging (DWI), which consists of segmenting the readout into multiple shots, holds a great potential for high resolution diffusion imaging as compared to single-shot imaging. It is shown to be less sensitive to magnetic field inhomogeneities and induces less off-resonance distortions [4]. However, coherent bulk motion during the application of the diffusion sensitizing gradients, can introduce phase shifts in the acquired signal. Rigid motion (involving translation and rotation) causes linearly varying phase maps, while non-rigid motion, such as brain pulsatile motion, may lead to non-linear phase variations [5]. In a multi-shot EPI acquisition, these phase maps may change from shot to shot, as each shot corresponds with a different excitation and each readout experiences a different phase corruption. If not corrected for, the shot-to-shot phase inconsistency may lead to image-space ghosting artifacts [6].

Various methods have been proposed to correct for phase related artifacts in multi-shot DWI. A common approach is to acquire an additional low-resolution navigator scan with the same diffusion weighting as during the high resolution scan, where it is assumed that the spins experience the same phase errors in both scans. The navigator scan can then be used to correct the motion-induced phase errors in the image space before the EPI shots are combined [7]. Alternatively, the phase map can be estimated retrospectively from the data to avoid the acquisition of additional navigator data. This can be done using a self-navigated acquisition scheme such as PROPELLER [8] or EPIK [9], or by exploiting the structured low-rank property of multi-shot DW data or a slowly varying phase map [10].

In this paper, we propose Accelerated Diffusion EPI with multi-contrast shoTs (ADEPT). ADEPT consists of a joint model-based reconstruction and parameter estimation framework and accompanying image acquisition strategy that allows accelerated dMRI by varying the diffusion contrast settings for each shot in a multi-shot acquisition, introducing intra-scan modulation. From the multi-contrast k-space data, in which each EPI shot is encoded with a different contrast weighting, the parameters of a diffusion tensor model are directly estimated, thereby surpassing the intermediate image reconstruction step of the conventional dMRI approach. To account for the phase mismatch between different shots, ADEPT estimates the phase map parameters for each shot (assuming a linear model) jointly with diffusion tensor parameter maps. Through Monte Carlo simulations, ADEPT is evaluated in terms of accuracy and precision and shown to outperform the conventional two-step diffusion parameter estimation approach.

*This project has received funding from the European Union's Horizon 2020 research and innovation program under the Marie Sklodowska-Curie grant agreement No 764513. The authors also acknowledge support of the European Space Agency (ESA) and BELSPO Prodex, and the Research Foundation Flanders (FWO Belgium) through project funding G084217N and 12M3116N.

[1]imec-Vision Lab, Dept. Physics, Univ. Antwerp, Antwerp, Belgium
[2]BIGR, Erasmus MC, Rotterdam, The Netherlands
[3]μNEURO Research Centre of Excell., Univ. Antwerp, Antwerp, Belgium

II. THEORY AND METHODS

This section describes the signal model of intra-scan modulated multi-shot diffusion data and introduces the ADEPT framework for joint diffusion tensor and phase parameter estimation.

A. DIFFUSION SIGNAL MODEL

Considering intra-scan modulated multi-shot EPI acquisition, where each shot of a multi-coil, multi-shot acquisition in the k-space is acquired with a different diffusion weighting, we can model the measured vectorized k-space diffusion data $\boldsymbol{q}_{n,c} \in \mathbb{C}^{n_k \times 1}$ of the c-th coil ($c \in \{1, \cdots, n_c\}$) and n-th shot ($n \in \{1, \cdots, n_s\}$), with n_k the number of k-space samples per shot, n_c the number of coil channels and n_s the total number of shots, as:

$$\boldsymbol{q}_{n,c} = \boldsymbol{A}_n \mathscr{F} \boldsymbol{C}_c \boldsymbol{f}_n + \boldsymbol{e} \quad , \tag{1}$$

with $\boldsymbol{f}_n \in \mathbb{C}^{n_v \times 1}$ the vectorized underlying noise free, fully sampled, DW image, defined on the grid points $\boldsymbol{r} = (r_x(j), r_y(j)) \in \mathbb{R}^{n_v \times 2}$, with n_v the number of voxels in the image, and $\boldsymbol{A}_n \in \{0,1\}^{n_k \times n_v}$, $\mathscr{F} \in \mathbb{C}^{n_v \times n_v}$, $\boldsymbol{C}_c \in \mathbb{C}^{n_v \times n_v}$ linear operators that describe the binary sampling mask corresponding to the n-th shot, the Discrete Fourier Transform operator and a diagonal matrix representing the coil sensitivity map of the c-th coil, respectively. Furthermore, $\boldsymbol{e} \in \mathbb{C}^{n_k \times 1}$ is a complex valued, additive noise contribution that can be modeled as a zero mean, complex, Gaussian random variable.

Let $\boldsymbol{S}_0 = (S_0(j)) \in \mathbb{C}^{n_v \times 1}$ denote the vectorized, complex-valued, non-DW image, which includes time-invariant phase components (caused by, for example, B_0 and B_1 field inhomogeneities, chemical shifts, or susceptibility differences). Then, adopting the diffusion tensor imaging (DTI) model, the DW image $\boldsymbol{f}_n$ with DW factor b_n and diffusion gradient direction $\boldsymbol{g}_n = (g_{nx}, g_{ny}, g_{nz})^T$ can be modeled for each voxel as:

$$f_n(j) = S_0(j) e^{-\boldsymbol{b}_n^T \boldsymbol{D}(j)} e^{i\phi_n(j)} \quad , \tag{2}$$

with $\boldsymbol{b}_n = b_n(g_{nx}^2, 2g_{nx}g_{ny}, 2g_{nx}g_{nz}, g_{ny}^2, 2g_{ny}g_{nz}, g_{nz}^2)^T \in \mathbb{R}^{6\times 1}$ a vector of the independent components of the 3×3 symmetric DW b-matrix, $\boldsymbol{D}(j) = (d_{xx}(j), d_{xy}(j), d_{xz}(j), d_{yy}(j), d_{yz}(j), d_{zz}(j))^T \in \mathbb{R}^{6\times 1}$ the vectorized, 3×3 symmetric diffusion tensor, and $\phi_n(j)$ the phase contribution that accounts for the effect of coherent bulk motion during the application of the diffusion sensitized gradients. If the motion is assumed to be rigid, the corresponding phase maps in the image space for each shot of the multi-shot EPI acquisition will be linear and can be voxel-wise modeled as follows [11]:

$$\phi_n(j) = \theta_{n0} + \theta_{n1} r_x(j) + \theta_{n2} r_y(j) \quad , \tag{3}$$

with θ_{n0} and $(\theta_{n1}, \theta_{n2})$ the offset and slope parameters of the motion-induced phase map, respectively.

B. JOINT PARAMETER ESTIMATION

Let $\overline{\boldsymbol{D}} = (\boldsymbol{D}^T(1), \cdots, \boldsymbol{D}^T(n_v))^T \in \mathbb{R}^{6n_v \times 1}$ denote the vector of symmetric diffusion tensors of all voxels. Furthermore, let $\overline{\boldsymbol{\theta}} = (\boldsymbol{\theta}_1^T, \cdots, \boldsymbol{\theta}_{n_s}^T)^T \in \mathbb{R}^{3n_s \times 1}$ be the motion-induced phase map parameter vector of all shots, where $\boldsymbol{\theta}_n = (\theta_{n0}, \theta_{n1}, \theta_{n2})^T$ is the motion-induced phase map parameter vector of the n-th shot. Assuming the non-DW image, $\boldsymbol{S}_0$, is estimated along with the diffusion and phase parameters, then the joint least squares estimator of $\boldsymbol{S}_0$, $\overline{\boldsymbol{D}}$ and the linear phase parameters $\overline{\boldsymbol{\theta}}$ from the multi-shot multi-contrast k-space data is given by:

$$\widetilde{\boldsymbol{D}}, \widetilde{\boldsymbol{S}}_0, \widetilde{\boldsymbol{\theta}} = \arg\min_{\overline{\boldsymbol{D}}, \boldsymbol{S}_0, \overline{\boldsymbol{\theta}}} \left(\sum_{n,c} || \boldsymbol{q}_{n,c} - \boldsymbol{A}_n \mathscr{F} \boldsymbol{C}_c \boldsymbol{f}_n(\overline{\boldsymbol{D}}, \boldsymbol{S}_0, \boldsymbol{\theta}_n) ||_2^2 \right) , \tag{4}$$

The large-scale optimization problem (4) is a non-linear least squares problem which can be solved using the cyclic Block Coordinate Descent (cBCD) [12] method. This method allows to divide the main problem (4) into two less complex sub-problems that are solved alternately in an iterative scheme. In the first sub-problem, the cost function is minimized with respect to $\overline{\boldsymbol{D}}$ and $\boldsymbol{S}_0$,

$$\widetilde{\boldsymbol{D}}^{t+1}, \widetilde{\boldsymbol{S}}_0^{t+1} = \arg\min_{\overline{\boldsymbol{D}}, \boldsymbol{S}_0} \left(\sum_{n,c} || \boldsymbol{q}_{n,c} - \boldsymbol{A}_n \mathscr{F} \boldsymbol{C}_c \boldsymbol{f}_n(\overline{\boldsymbol{D}}, \boldsymbol{S}_0, \widetilde{\boldsymbol{\theta}}_n^t) ||_2^2 \right) , \tag{4.A}$$

whereas in the second sub-problem the cost function minimized with respect to phase parameter vector, $\overline{\boldsymbol{\theta}}$,

$$\widetilde{\boldsymbol{\theta}}^{t+1} = \arg\min_{\overline{\boldsymbol{\theta}}} \left(\sum_{n,c} || \boldsymbol{q}_{n,c} - \boldsymbol{A}_n \mathscr{F} \boldsymbol{C}_c \boldsymbol{f}_n(\widetilde{\boldsymbol{D}}^{t+1}, \widetilde{\boldsymbol{S}}_0^{t+1}, \boldsymbol{\theta}_n) ||_2^2 \right) , \tag{4.B}$$

Each sub-problem is solved using the trust region Newton algorithm combined with Powell's dog leg method [13]. The sub-problems (4.A) and (4.B) are initialized at $\overline{\boldsymbol{D}} = \widetilde{\boldsymbol{D}}^t$, $\boldsymbol{S}_0 = \widetilde{\boldsymbol{S}}_0^t$ and $\overline{\boldsymbol{\theta}} = \widetilde{\boldsymbol{\theta}}^t$, respectively, with $\widetilde{\boldsymbol{D}}^0 = \overline{\boldsymbol{D}}_{ini}$, $\widetilde{\boldsymbol{S}}_0^0 = \boldsymbol{S}_{0,ini}$ and $\widetilde{\boldsymbol{\theta}}^0 = \overline{\boldsymbol{\theta}}_{ini}$ the initial values of the parameters. Since both (4.A) and (4.B) are non-convex optimization problems, they can contain multiple local minima. For this reason, a proper initialization of the cBCD algorithm is vital to find the global minimum. These initial values are found using a SENSE reconstruction and estimation (SENSE-re) approach where first, DW images are reconstructed separately for each shot by performing SENSE reconstruction [14] using the BART toolbox [15]. Next, the DTI parameters and non-DW image are estimated per voxel from the reconstructed magnitude images and their values are used as initial values in the cBCD approach ($\overline{\boldsymbol{D}}_{ini}$, $\boldsymbol{S}_{0,ini}$). The initial values for the phase parameters ($\overline{\boldsymbol{\theta}}_{ini}$) are estimated by fitting (3) to the phase maps of the individually SENSE reconstructed images.

III. EXPERIMENTS

To evaluate the accuracy and precision with which ADEPT can estimate diffusion tensor parameters from multi-contrast multi-shot data in the presence of shot-to-shot phase variations, Monte Carlo simulation experiments were performed. For this purpose, multi-shot multi-coil k-q-space data was generated using the models (1) and (2). As ground truth parameters, a 96×96 diffusion tensor map and non-DW magnitude image, which were both estimated from a real

diffusion MRI dataset, were used. The phase of the (fully sampled) non-DW image was assumed to be known.

The simulated k-q-space data consisted of $n_s = 64$ (4 non-DW and 60 DW) EPI shots (b-value=1.15 $ms/\mu m^2$), each with a different gradient direction (distributed uniformly over a sphere). For each of the 60 DW shots, a different linear phase map was generated according to (3). The offset and slope ground truth phase parameters θ_0, θ_1 and θ_2 were drawn from zero-mean Gaussian distributions with standard deviation π, $\pi/r_x(n_v)$ and $\pi/r_y(n_v)$, respectively. Furthermore, the number of coils was set to $n_c = 8$ and the coil sensitivity maps from a multi-coil scan were used to simulate the diffusion k-space data.

To construct the 64 shots, fully sampled k-space data was generated for each shot, which was then retrospectively under-sampled by applying an under-sampling mask. Four different masks were used, where each mask samples the central four lines of the k-space, whereas the non-central part of the k-space is sub-sampled with a factor 4, as illustrated in Fig. 1. Together, the four masks cover the whole k-space. Each of the four masks was applied to the fully sampled k-space data of i) the non-DW image, and ii) 15 out of the 60 differently DW images. Finally, the multi-shot data was corrupted by additive, complex valued, zero mean, Gaussian white noise. The noise standard deviation was chosen to obtain Signal to Noise Ratio (SNR) values in the range $[10,\cdots,50]$, where the SNR is defined in image space as the ratio of the spatial average of the noiseless, fully sampled, non-DW image of one coil channel and the standard deviation of the noise. For each SNR level, $n_r = 20$ realizations of noisy data were generated for statistical analysis.

The diffusion parameters, $\overline{\boldsymbol{D}}$, the magnitude of the non-DW image, $\boldsymbol{S}_0$, and linear phase parameters, $\overline{\boldsymbol{\theta}}$, were then estimated from each noisy realization using SENSE-re and our proposed approach, ADEPT. To improve parameter estimation robustness, background voxels were excluded by defining a selection mask obtained by thresholding the non-DW image based on the SNR [16]. The estimation performance of both methods was evaluated using the following quantitative performance measures: *bias*, defined as $\bar{\hat{x}} - x$, where $\bar{\hat{x}}$ is the sample mean of the n_r parameter estimates $\hat{x}$ with ground truth value x, standard deviation (std), defined as $[\Sigma(\hat{x}-\bar{\hat{x}})^2/(n_r-1)]^{1/2}$ and root mean square error (RMSE), defined as $[(\hat{x}-x)^2]^{1/2}$. For both methods, these measures were calculated per voxel for Mean Diffusivity (MD) and Fractional Anisotropy (FA). Next, the spatial means of the masked region for the thus obtained bias, std and RMSE maps were calculated. Furthermore, the accuracy and precision of the ADEPT phase parameter estimates were evaluated by calculating their RMSE.

IV. RESULTS

Fig. 2 shows MD (top) and FA (bottom) maps estimated from a simulated dataset acquired with the 4-shot multi-contrast EPI sequence described in section III with $SNR = 20$. Estimated maps using SENSE-re (middle) are compared to those obtained with ADEPT (right), where the ground truth MD and FA maps (left) are shown as a reference. Fig. 3 shows the estimated bias, standard deviation and RMSE maps of both methods for MD (top) and FA (bottom) as calculated from the Monte Carlo simulation experiment described in the previous section with $SNR = 20$. Fig. 4 shows the spatial means of the bias, standard deviation and RMSE maps calculated for different SNR levels. Fig. 5 shows the RMSE (averaged over the shots) of the phase parameters estimated using ADEPT and estimated by fitting (3) to the SENSE-re reconstructed images.

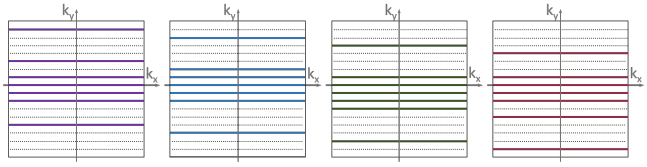

Fig. 1. K-space sampling patterns of the individual shots of the 4-shot EPI acquisition. The different colors represent different diffusion contrasts.

V. DISCUSSION

Fig. 2 shows that the diffusion parameter maps estimated with SENSE-re (middle) look noisier than those estimated by ADEPT (right), which is also reflected in the higher bias, std and RMSE values observed in Fig. 3 and Fig. 4. ADEPT's superior accuracy and precision may be partly attributed to its capacity to accurately estimate the phase parameters, as demonstrated in Fig. 5.

The current work has some limitations that will be addressed in future work. First of all, ADEPT still has to be compared with other state of the art methods and evaluated in in-vivo data. Furthermore, ADEPT can be extended to include more complex phase models than the linear model considered in this work. Finally, the intra-scan modulated acquisition framework of ADEPT has many degrees of freedom which can be but have not yet been fully exploited by applying statistical experiment design, allowing to find the settings that maximize the precision of the estimated diffusion parameters [17].

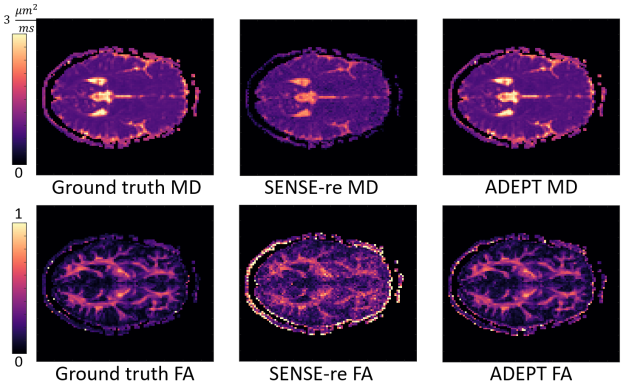

Fig. 2. Estimated MD (top) and FA (bottom) maps for a dataset with $SNR = 20$. The ground truth values (left) are shown along with the SENSE-re (middle) and ADEPT (right) results.

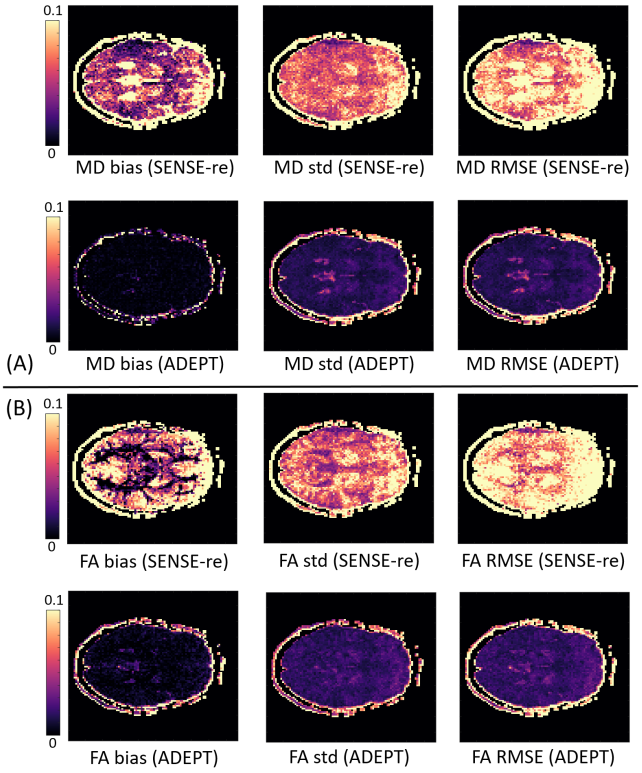

Fig. 3. Bias (left), standard deviation (middle) and RMSE (right) maps of MD (A), and FA (B) estimated with SENSE-re and ADEPT from datasets with $SNR = 20$.

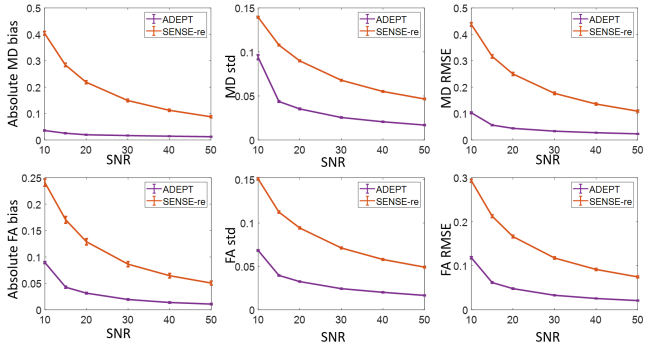

Fig. 4. Spatial averages of the absolute bias (left), standard deviation (middle) and RMSE (right) of MD (top) and FA (bottom) estimated with ADEPT and SENSE-re for multiple SNR levels.

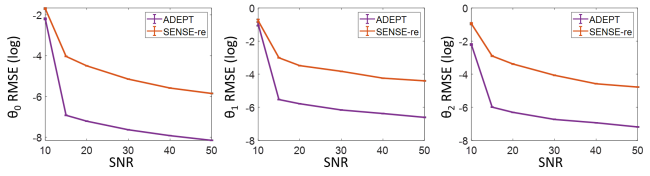

Fig. 5. RMSE of the estimated phase parameters θ_0 (left), θ_1 (middle) and θ_2 (right) of ADEPT and SENSE-re. The RMSE values, averaged across the shots, are shown for multiple SNR levels.

VI. CONCLUSION

We presented ADEPT, a framework that allows robust estimation of diffusion parameters in multi-shot EPI studies, while enabling accelerated imaging. Using joint information of all the differently diffusion weighted shots and simultaneously estimating phase map parameters, ADEPT allows for more accurate and precise estimation of the diffusion parameters compared to more conventional image space methods, as was shown by extensive simulation experiments.

REFERENCES

[1] C. L. Welsh, E. V. Dibella, G. Adluru, and E. W. Hsu, "Model-based reconstruction of undersampled diffusion tensor k-space data," *Magnetic Resonance in Medicine*, vol. 70, no. 2, pp. 429–440, 2013.

[2] Y. Zhu, X. Peng, Y. Wu, E. X. Wu, L. Ying, X. Liu, H. Zheng, and D. Liang, "Direct diffusion tensor estimation using a model-based method with spatial and parametric constraints," *Medical Physics*, vol. 44, no. 2, pp. 570–580, 2017.

[3] Z. Dong, E. Dai, F. Wang, Z. Zhang, X. Ma, C. Yuan, and H. Guo, "Model-based reconstruction for simultaneous multislice and parallel imaging accelerated multishot diffusion tensor imaging," *Medical Physics*, vol. 45, no. 7, pp. 3196–3204, 2018.

[4] D. Le Bihan, C. Poupon, A. Amadon, and F. Lethimonnier, "Artifacts and pitfalls in diffusion MRI," *Journal of Magnetic Resonance Imaging*, vol. 24, no. 3, pp. 478–488, sep 2006.

[5] M. Mani, M. Jacob, D. Kelley, and V. Magnotta, "Multi-shot sensitivity-encoded diffusion data recovery using structured low-rank matrix completion (MUSSELS)," *Magnetic Resonance in Medicine*, vol. 78, no. 2, pp. 494–507, 2017.

[6] X. Ma, Z. Zhang, E. Dai, and H. Guo, "Improved multi-shot diffusion imaging using GRAPPA with a compact kernel," *NeuroImage*, vol. 138, pp. 88–99, sep 2016.

[7] H.-K. Jeong, J. C. Gore, and A. W. Anderson, "High-resolution human diffusion tensor imaging using 2-D navigated multishot SENSE EPI at 7 T," *Magnetic Resonance in Medicine*, vol. 69, no. 3, pp. 793–802, mar 2013.

[8] J. G. Pipe, V. G. Farthing, and K. P. Forbes, "Multishot diffusion-weighted FSE using PROPELLER MRI," *Magnetic Resonance in Medicine*, vol. 47, no. 1, pp. 42–52, 2002.

[9] R. G. Nunes, P. Jezzard, T. E. J. Behrens, and S. Clare, "Self-navigated multishot echo-planar pulse sequence for high-resolution diffusion-weighted imaging," *Magnetic Resonance in Medicine*, vol. 53, no. 6, pp. 1474–1478, jun 2005.

[10] N. K. Chen, A. Guidon, H. C. Chang, and A. W. Song, "A robust multi-shot scan strategy for high-resolution diffusion weighted MRI enabled by multiplexed sensitivity-encoding (MUSE)," *NeuroImage*, vol. 72, pp. 41–47, may 2013.

[11] I. Rabanillo, S. Sanz-Estébanez, S. Aja-Fernández, J. Hajnal, C. Alberola-López, and L. Cordero-Grande, "Joint image reconstruction and phase corruption maps estimation in multi-shot echo planar imaging," in *Computational Diffusion MRI*, E. Bonet-Carne, F. Grussu, L. Ning, F. Sepehrband, and C. M. W. Tax, Eds. Cham: Springer International Publishing, 2019, pp. 19–27.

[12] A. Beck and L. Tetruashvili, "On the convergence of block coordinate descent type methods," *SIAM Journal on Optimization*, vol. 23, no. 4, pp. 2037–2060, 2013.

[13] Y. Yuan, "Conditions for convergence of trust region algorithms for nonsmooth optimization," *Mathematical Programming*, vol. 31, no. 2, pp. 220–228, 1985.

[14] K. P. Pruessmann, M. Weiger, M. B. Scheidegger, and P. Boesiger, "SENSE: Sensitivity encoding for fast MRI," *Magnetic Resonance in Medicine*, vol. 42, no. 5, pp. 952–962, nov 1999.

[15] J. I. Tamir, F. Ong, J. Y. Cheng, M. Uecker, and M. Lustig, "Generalized Magnetic Resonance Image Reconstruction using The Berkeley Advanced Reconstruction Toolbox," ISMRM Workshop on Data Sampling and Image Reconstruction, Sedona 2016.

[16] J. Sijbers, B. Vanrumste, G. Van Hoey, P. Boon, M. Verhoye, A. Van Der Linden, and D. Van Dyck, "Automatic localization of EEG electrode markers within 3D MR data," *Magnetic Resonance Imaging*, vol. 18, no. 4, pp. 485–488, may 2000.

[17] A. van den Bos, *Parameter Estimation for Scientists and Engineers*. Hoboken, NJ, USA: John Wiley Sons, Inc., jun 2007.